Coherence in the turbulent cascade

By Javier Jiménez[1]

1. Motivation and objectives

It has been known for some time that intermittency is an inevitable consequence of multiplicative cascades, which arise naturally from two assumptions (Jiménez 1999):

1. Causal locality, which implies that a variable v_n, associated with the cascade step n, depends *only* on the value of a single 'parent' in the preceding cascade step so that its probability distribution p_n is

$$p_n(v_n) = \int W(v_n|v_{n-1};\, n) p_{n-1}(v_{n-1})\, \mathrm{d}v_{n-1}. \tag{1}$$

   This is in contrast to more complicated functional dependencies such as on the values of v_{n-1} in some extended spatial neighborhoods or on several previous cascade stages.

2. Scale similarity, which implies that the transition probability distribution W is independent of the cascade step n and depends only on the ratio v_n/v_{n-1}.

The model assumes that each step generates eddies with smaller length scales Δx, usually $\Delta_0 2^{-n}$. After the initial effects are forgotten, the probability distribution of v_n is completely determined by the distribution W of the 'breakdown coefficients' v_n/v_{n-1} (Frisch, 1995). These assumptions are known to describe well some of the statistical properties of isotropic turbulence and, in particular, the scaling exponents of the velocity structure functions (Meneveau & Sreenivasan, 1991),

$$S_p = \langle |\Delta u_{\Delta x}|^p \rangle \sim \Delta x^{\zeta_p}, \tag{2}$$

where $\langle\rangle$ stands for global averaging, and

$$\Delta u_{\Delta x} = u(x + \Delta x/2) - u(x - \Delta x/2). \tag{3}$$

This is so even if there is no precise implied dynamical model of how the multiplicative process is related to the Navier-Stokes equations (Jiménez 1998).

The converse of the previous discussion is not true, and intermittency does not necessarily imply a multiplicative cascade. Structural observations of numerical and experimental turbulent flows show, for example, that the vorticity is partially organized into coherent filaments with large aspect ratios, whose lifetimes are long

1 Also with the School of Aeronautics, U. Politécnica Madrid.

compared to those which would correspond to their smallest dimensions (Jiménez & Wray, 1998). The concept of 'scale' is difficult to apply to these anisotropic structures, and several models have been proposed in which the flow is described in terms of self-similar and coherent components.

It was argued by Jiménez and Wray (1998) and Jiménez (1999) that this differentiation into components is a natural consequence of intermittency itself and that any intermittent *field*, as opposed to a set with no spatial topology, is likely to develop a coherent component which is essentially different from the background. This is because the first of the two assumptions above is violated, and the evolution of the field variable generically depends on global, besides local, information. The nonlocality of the interactions introduces the average intensity of the fluctuations as an extra scale for the cascade, self-similarity is lost, and strong structures behave differently from weaker ones. Thus, while self-similarity is natural for noninteracting variables, it is not a generic behavior for fields in which several elements at the same stage of the cascade are coupled to each other.

In such cases, such as in three-dimensional turbulence, a full description of the strong structures should include their geometry, which controls how they interact with the background, but this has only been possible at the moderate Reynolds numbers accessible by numerical simulations. Such flows have very short inertial ranges, and it is difficult in them to study structures whose dimensions are neither in the dissipative nor in the integral range of scales. This was nevertheless the way in which vortex filaments with diameters of the order of the Kolmogorov scale were first identified. Only later could similar signals be educed from experimental flows at higher Reynolds numbers. A summary was given by Jiménez (1998).

It was argued theoretically by Jiménez and Wray (1998) that these dissipation-scale structures should only be the most obvious manifestations of coherence and that a continuum of both weaker and stronger ones should be expected. The former would have larger diameters and weaker vortices and could perhaps be related to the low-pressure filaments observed in some experiments (Cadot, Douady & Couder, 1995). The latter would have diameters below the Kolmogorov scale and velocity differences comparable to those of the presently observed vorticity filaments. Reliable numerical and experimental data are lacking for the sub-Kolmogorov scales, but the purpose of this note is to discuss whether evidence can be found in the available experiments for, or against, organized structures in the inertial range of scales.

Experimental data are analyzed in the next section, of which a more extended version can be found in (Jiménez *et al.*, 1999). The structure of filtered direct numerical simulation fields is briefly described in §3, and conclusions are offered in §4.

2. Analysis of experimental data

The scaling properties of the inertial range have traditionally been characterized by the probability density functions (p.d.f.s) of the velocity differences at different

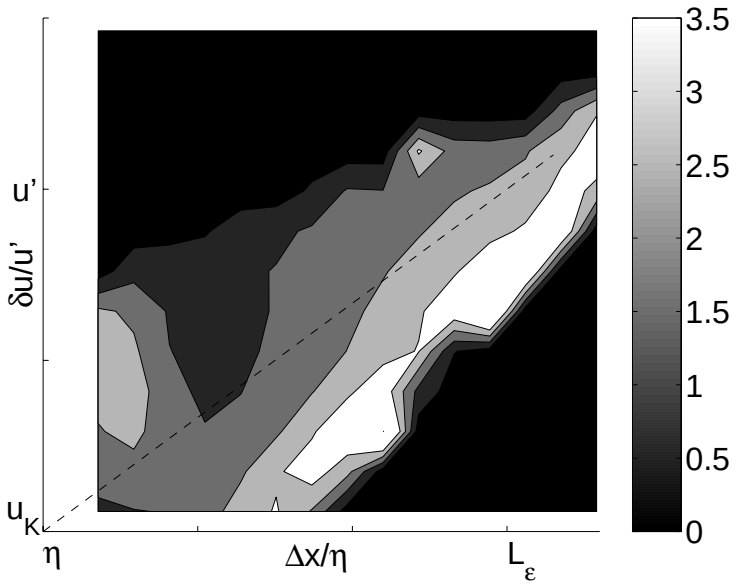

FIGURE 1. Midpoint value of the conditional p.d.f.s of the breakdown coefficients for the surrogate averaged dissipation, as a function of the averaging length and of the 'parent' velocity increment. $Re_\lambda = 1600$. The diagonal dashed line represents the standard Kolmogorov cascade.

separations and, in particular, by their structure functions. It has been repeatedly noted, however, that statistical moments are poor discriminants of the differences between probability distributions (Chhabra & Sreenivasan, 1992; Nelkin, 1995; Jiménez *et al.*, 1999), so that, even if is found that the structure functions scale approximately as powers, as in Eq. (2), it is difficult to conclude from that observation that the p.d.f.s of the breakdown coefficients are truly independent of the length scale.

Here we directly study the probability distributions, using three time series of the longitudinal velocity component in approximately isotropic turbulence in low-temperature helium gas (Belin *et al.*, 1997). The Reynolds numbers are $Re_\lambda = 155$, 760, and 1600. The range between the integral length L_ε and the Kolmogorov scale η is $8,400$ at the highest Reynolds number, and each set contains $10^4 - 10^5$ integral scales. For more details, see Jiménez *et al.* (1999). Only the two highest Reynolds numbers have clear power-law ranges in their spectra, and they are the ones used below. The remaining set, whose Reynolds number is comparable to those of numerical simulations, does not collapse well with them.

We first discuss the p.d.f.s of the breakdown coefficients

$$W(q_{2\Delta x}) = W(\varepsilon_{\Delta x}/2\varepsilon_{2\Delta x}) \tag{4}$$

for the averaged dissipation

$$\varepsilon_{\Delta x} = \frac{1}{\Delta x}\int_{x-\Delta x/2}^{x+\Delta x/2} (\partial_x u)^2 \,\mathrm{d}x. \tag{5}$$

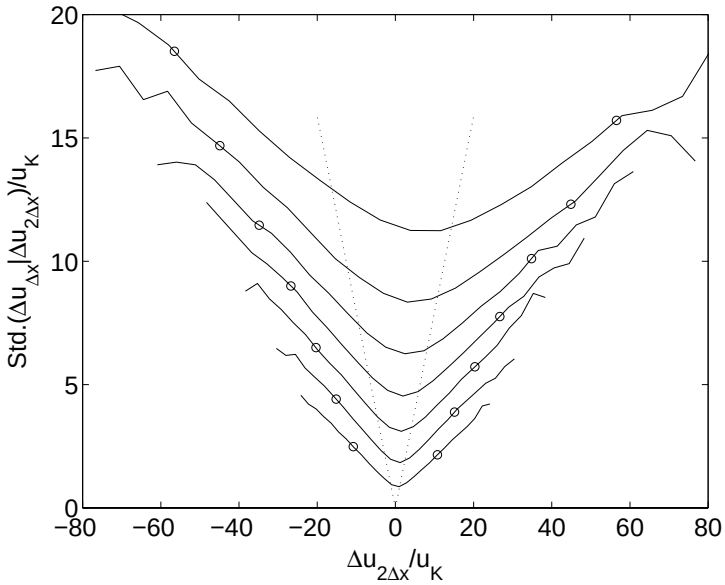

FIGURE 2. Standard deviation of the conditional distributions of the velocity increments, as a function of the separation and velocity increments of their 'parent' intervals. Each line represents a logarithmically spaced separation in the range $2\Delta x/\eta = 25(\times 2)1600$, increasing upwards, and is normalized with the global Kolmogorov velocity scale $u_k = \nu/\eta$. The dotted lines would correspond to complete self similarity of the cascade, and the open circles are the abscissae of the velocity thresholds used to compute Fig. 3(a). $Re_\lambda = 1600$.

They are roughly symmetrical in (0, 1) and approximately bell-shaped. It was suggested by Van Atta and Yeh (1975) that they can be characterized by their mid-point values, $W(0.5)$, which is where their maxima approximately occur. This value varies with the separation (Van Atta & Yeh, 1975) and with the dissipation in the parent interval, arguing against strict self-similarity of the cascade, and is given in Fig. 1. It is seen that the weakest fluctuations at each length scale have narrower distributions with taller peaks, implying that they break down into sub-segments whose dissipations tend to be half of that of their parents, as would be expected in an incoherent situation in which the parent is composed of several uncorrelated smaller pieces. More intense fluctuations have more spread distributions with lower central peaks, suggesting coherence. This effect is most pronounced at the smallest scales.

Another way of characterizing the cascade is to directly study the conditional probability distributions of the velocity increments as a function of the velocity increments of their parent intervals. This was done by Jiménez *et al.* (1999) for the data sets discussed here. If the cascade were completely self-similar, the conditional p.d.f.s would be universal, and their means and standard deviations would be proportional to the velocity increment of the parent interval,

$$\langle \Delta u_{\Delta x} | \Delta u_{2\Delta x} \rangle = \Delta u_{2\Delta x}/2, \qquad \langle \Delta u_{\Delta x}^2 | \Delta u_{2\Delta x} \rangle = \Delta u_{2\Delta x}^2/2^{2/3}. \tag{6}$$

The second relation assumes Kolmogorov's inertial scaling for the energy spectrum.

The first relation in Eq. (6) is approximately satisfied by the data, but the second one is not, and the form of the conditional distributions depends on Δx. The conditional standard deviations are given in fig. 2 for several separations in the inertial range. The dotted lines are Eq. (6) and do not describe the experiments well. The measured deviations are bounded below by a global additive 'noise' which is of the order of the Kolmogorov velocity scale at that particular separation, $(\varepsilon\Delta x)^{1/3}$. This is consistent with the idea introduced above that the breakdown of the weak fluctuations is controlled by the background. The situation is different for the stronger fluctuations, whose intensities depend more linearly on the velocity differences of their parent intervals. It was shown by Jiménez *et al.* (1999) that it is possible to approximately describe Fig. 2 as the superposition of a random additive process, corresponding to the minimum conditional standard deviation at each separation and a multiplicative one that generates the linear tails. A similar conclusion was reached by Friedrich and Peinke (1997).

Several refinements of this analysis are possible. It was, for example, noted by Jiménez *et al.* (1999) that velocity increments are used in this context as band-pass filters to isolate a range of length scales and that sharper filters could give different results. It was also remarked by Sreenivasan and Dhruva (1998) that this and other flows are not isotropic and that the scaling improves if this is taken into account by analyzing increments associated with a given mean velocity. Both corrections were tested here, the former by using a five-point band-pass filter instead of (3), and the latter by repeating the analysis only for those segments for which the mean velocity is in a narrow range around the global mean. Figure 2 is essentially unchanged by both corrections.

2.1. Educed velocity traces

To gain some understanding of the approximately self-similar intense structures implied by the linear tails of Fig. 2, we compiled averaged velocity traces conditioned on strong velocity increments across a given distance. Some precautions had to be taken to avoid the smearing that would result from counting each structure more than once. Disjoint 'active' segments were defined, each of which was the largest connected union of segments of width Δx for which $\Delta u_{\Delta x} > u_{thr}$, where u_{thr} was fixed to a multiple of the global r.m.s. value of $\Delta u_{\Delta x}$. The velocities around the mid-points of all the active segments were then extracted and averaged together.

The resulting conditionally averaged velocities are shown in Fig. 3(a), for separations ranging from the dissipative to the integral range of length scales and for a relatively high conditioning u_{thr}. They are roughly antisymmetric with widths and intensities which are consistent with those of the conditioning algorithm. Somewhat similar traces were found by Belin *et al.* (1996) for the dissipative range and were interpreted by them as the effect of single vortices advected at an angle to the mean stream. In the present analysis the averaged structures in Fig. 3 are not representative of individual velocity traces and cannot be used directly to deduce the type of structures which are being observed.

Different traces can, in fact, be interpreted as caused by different structures. A hump of width δ and height u_δ is, for example, consistent with a positive vortex of

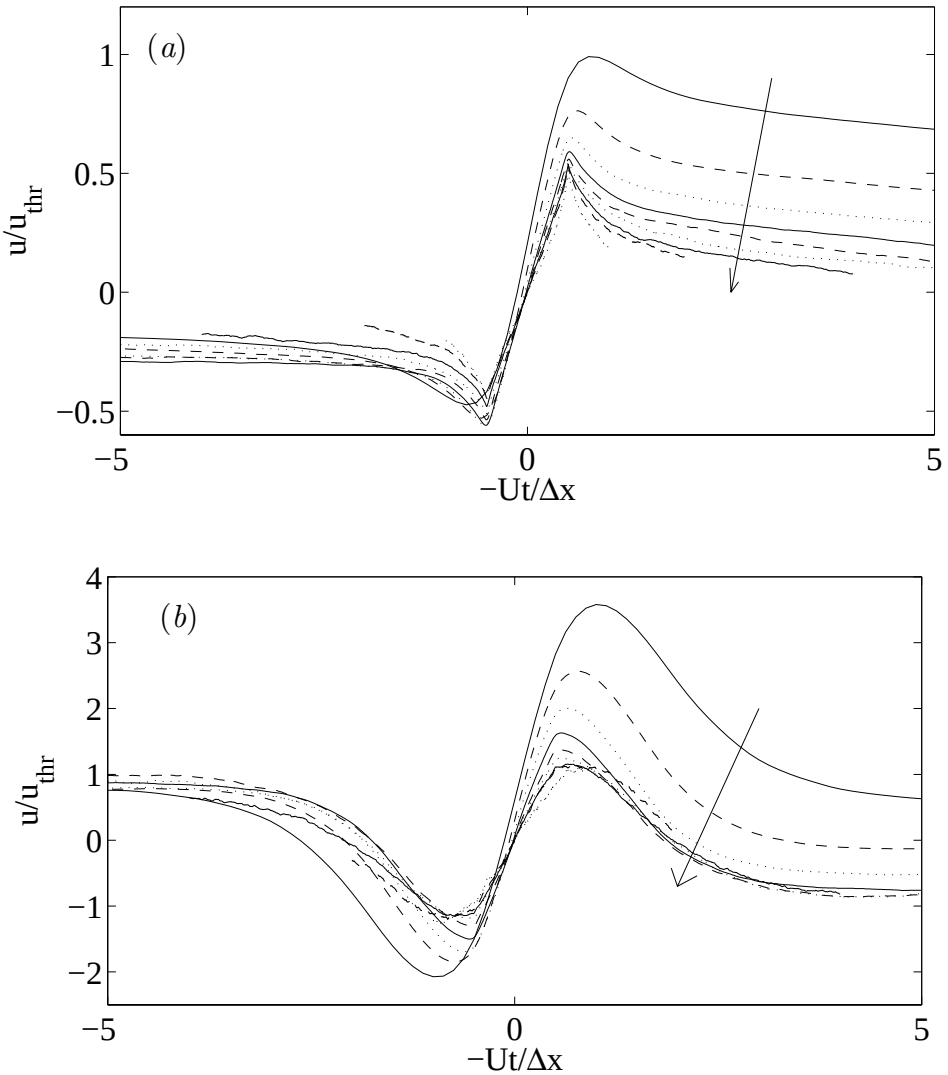

FIGURE 3. Mean velocity, conditioned on $\Delta u_{\Delta x} > u_{thr}$. Velocities and abscissae are normalized with the conditioning values, and $\Delta x/\eta = 12(\times 2)3000$, increasing in the direction of the arrow. $Re_\lambda = 1600$. (*a*) $u_{thr} = 3\langle \Delta u_{\Delta x}^2 \rangle^{1/2}$. These thresholds are given in Fig. 2. (*b*) $u_{thr} = 0.2\langle \Delta u_{\Delta x}^2 \rangle^{1/2}$.

circulation $2\pi\delta u_\delta$ passing at a distance $O(\delta)$ below the probe (or with a negative one above it). A negative hump is also consistent with a vortex of the opposite sign. Because the detection algorithm always centers the structures about their positive slopes, negative humps precede the detector while positive ones lag behind it, and their average results in traces similar to those in Fig. 3. If those were the only types of traces found in our sample, the conditional average will return to the global mean value in a distance comparable to the detection length. That this is not so is due to the presence of velocity 'steps' which do not immediately return to the mean and which cannot be explained by vortices. The most likely interpretation of these steps are vortex sheets or plane stagnation strains. The three kinds of traces are found

in our sample, as well as others which are harder to interpret, and neither type is clearly dominant. The traces for the smaller separations are more asymmetric than those for the larger ones, which could be interpreted as an indication that sheets or stagnation structures become more common at the smaller scales.

The velocity thresholds used in this figure are plotted in Fig. 2 and fall in the approximately linear part of the conditional standard deviation curves. It was checked that the results are independent of the precise threshold as long as it falls in the linear part of the standard deviation curves. Conditional averages using a much lower threshold in the range of the background are given in Fig. 3(b). They quickly return to the mean outside the central detection interval $(-0.5, 0.5)$ and would, therefore, seem to imply the predominance of vortices among weak structures. Inspection of individual traces show that conclusion to be incorrect. The difference between the velocities selected by the two thresholds is that, while those at the higher threshold retain some coherence outside the detection interval and therefore produce mean values which are not trivially zero, those at weak thresholds do not, and the traces outside the detection interval are essentially random. Their average immediately returns to the global mean. The difference between the two sets of traces is, therefore, another measure of the higher coherence of the strong fluctuations as compared with the weaker ones.

4. Direct numerical simulations

Given the difficulties in interpreting the conditional velocity traces obtained from one-dimensional signals, it is tempting to compare them with the results of similar conditioning in three-dimensional direct numerical simulations even if their Reynolds numbers are lower. In this section we present two figures from an isotropic simulation at $Re_\lambda = 168$ (Jiménez & Wray, 1998), for which $L_\varepsilon/\eta = 290$. A plane section of the vorticity magnitude without filtering is shown in Fig. 4(a) and shows a complicated pattern of vortex sheets whose width is a few Kolmogorov scales. Detailed inspection shows that the most intense vorticity is in the form of circular vortices, some of which are associated to sheets, presumably corresponding to the filaments observed in three-dimensional visualizations (Jiménez & Wray, 1998).

To obtain an equivalent representation for the velocity differences, we define a 'discrete vorticity',

$$\Omega_{\Delta x,\,i} = \Delta x^{-1} \varepsilon_{ijk} \Delta u_{k,\,\Delta x_j}\,, \tag{7}$$

where ε_{ijk} is the fully antisymmetric unit tensor and the velocity increments replace the usual derivatives. That quantity, although not a true vector, is an approximation to the result of filtering the vorticity over a box of size Δx^3 and gives a sense of how the velocity increments separate into rotational and potential components. The magnitude of $\Omega_{\Delta x}$ is shown in Fig. 4(b) and is dominated by a strong 'vortex' at the location of the cross. It can be shown from three-dimensional representations that the most intense values of the discrete vorticity magnitude are organized into roughly tubular objects, although with smaller aspect ratios than those found in the dissipation range, and that 'vortex' lines of $\Omega_{\Delta x}$ run along their axes and connect neighboring objects as would be expected of true vortices. It can be tested

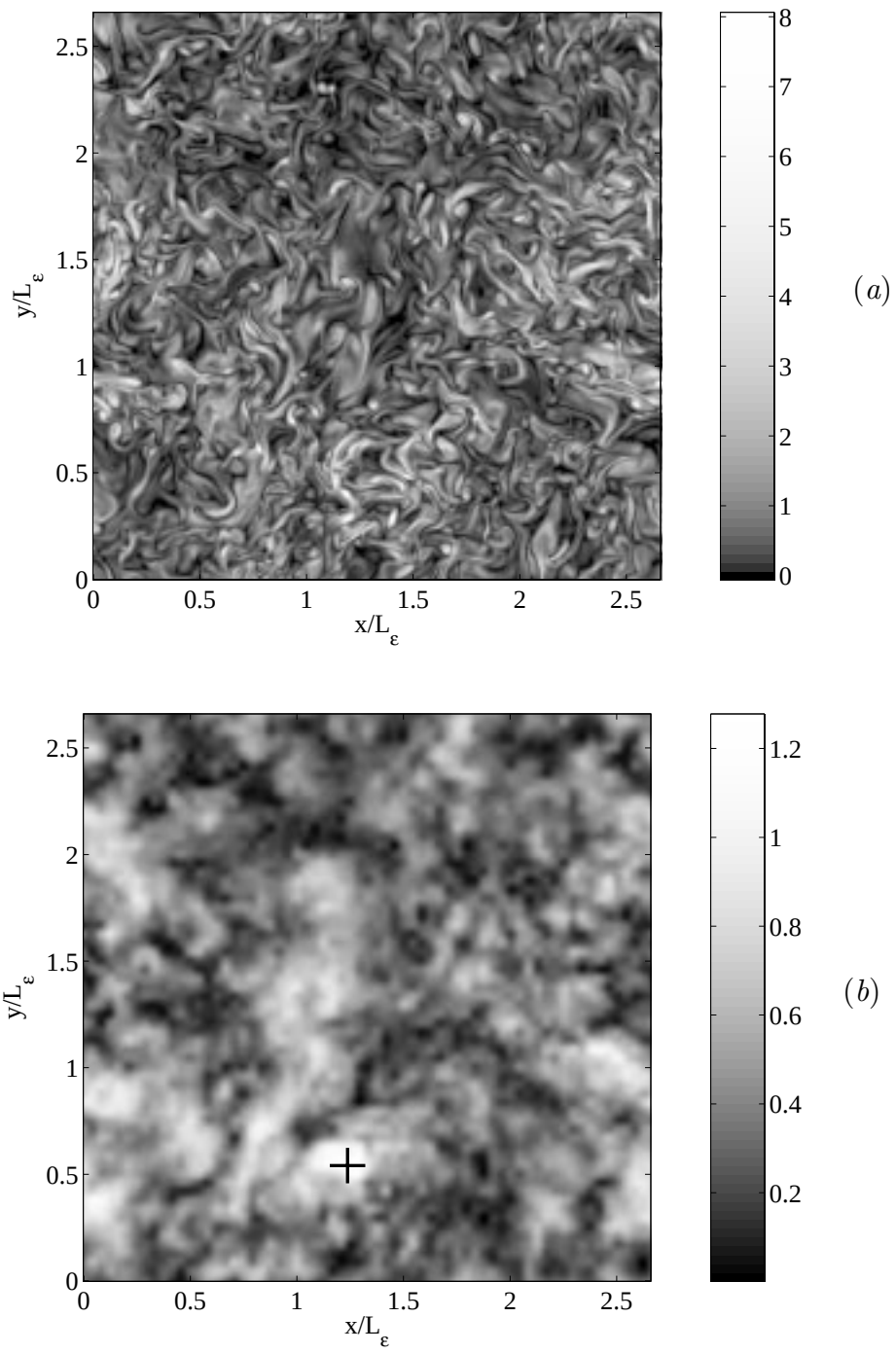

FIGURE 4. (*a*) Vorticity magnitude in a plane section across a triply periodic computational box of isotropic turbulence at $Re_\lambda = 170$ (Jiménez & Wray, 1998). The smallest visible features are approximately 2-3 Kolmogorov lengths across. (*b*) 'Discrete vorticity' magnitude in the same plane. The velocity increments are computed over $\Delta x/\eta = 50$, which is the size of black cross. The scale bars to the right are normalized with the global r.m.s. vorticity magnitude.

independently that a probe moving in the neighborhood of each of these objects, more or less perpendicularly to their axes, would see velocity increments at scale Δx which are consistent with the passage of a vortex, but a two-dimensional section of $\Delta u_{\Delta x}$ contains other structures which are difficult to explain in this way.

The comparison of the two parts of Fig. 4 shows that the discrete 'vortex' is not simply a smoothed version of a single dissipation-scale structure, but the collective effect of a particularly strong sheet and a cluster of smaller vortex cores.

5. Conclusions

We have shown that available experimental evidence is inconsistent with a strictly self-similar multiplicative cascade in the inertial range. A better description is that the velocity increments at scale Δx are related to those at their 'parent' intervals by the superposition of a local multiplicative process and of a 'global' additive noise whose intensity is proportional to the standard deviation of $\Delta u_{2\Delta x}$. This is consistent with the theoretical arguments outlined in the introduction, which suggest that this superposition is a generic property of cascades in *fields* and results in the separation of the field into weak and strong components with different behaviors. This separation is illustrated here by the conditional distributions of the breakdown coefficients of the dissipation, which are shown to depend on the relative intensity of their parent intervals with respect to their Kolmogorov-predicted average.

The implied cascade model is

$$v_{n+1} = v_n \phi_1 + \langle v_n^2 \rangle^{1/2} \phi_2, \tag{8}$$

where ϕ_1 and ϕ_2 are mutually independent stochastic processes. As far as we are aware, models of this type have seldom been considered in the literature although some related numerical experiments, in which the additive term is missing but the variance of ϕ_1 depends nonlinearly on $\langle v_n^2 \rangle^{1/2}$, were presented by Jiménez (1999). The case in which ϕ_1 is deterministic leads to a Fokker-Plank equation which may result in intermittency under the proper assumptions for ϕ_2 and which has been studied by Friedrich and Peinke (1997).

The multiplicative cascade is recovered for fluctuations which are much stronger than the background, and such fluctuations were studied both through conditional averaging and, to a lesser extend, through visualizations of numerical fields at lower Reynolds numbers. It was noted that the symmetry of the conditionally obtained averages is spurious and can be interpreted as the superposition of different structures that include both quasi-circular vortices and vortex or stagnation sheets. The latter seem to become more prevalent at smaller separations.

It is impossible with the present data to distinguish between the different structural models, but the comparison with the results of DNS suggests that inertial-scale structures, including vortices, exist and that at least some of them consist of clusters of smaller structures. The dynamics of the inertial range of scales, in isotropic turbulence or otherwise, is one of the greatest unknowns in our present understanding of turbulence. The ambiguities of the present study underline the need for high

Reynolds number experiments which are more complete than time traces of one velocity component.

This work was supported in part by the Spanish CICYT under contract PB95-0159, and by the Training and Mobility program of the EC under grant CT98-0175. Special thanks are due to A.A. Wray for reviewing a preliminary version of this manuscript.

REFERENCES

Belin, F., Maurer, J., Tabeling, P. & Willaime, H. 1996 Observation of intense filaments in fully developed turbulence. *J. Physique II.* **6,** 573-583.

Belin, F., Maurer, J., Tabeling, P. & Willaime, H. 1997 Velocity gradient distributions in fully developed turbulence: experimental study. *Phys. Fluids.* **9,** 3843-3850.

Cadot, O., Douady, S. & Couder, Y. 1995 Characterization of the low-pressure filaments in the three-dimensional turbulent shear flow. *Phys. Fluids.* **7,** 630-646.

Chhabra, A.B. & Sreenivasan, K.R. 1992 Scale invariant multipliers in turbulence. *Phys. Rev. Lett.* **68,** 2762-2765.

Friedrich, R. & Peinke, J. 1997 Description of a turbulent cascade by a Fokker-Plank equation. *Phys. Rev. Lett.* **78,** 863-866.

Frisch, U. 1995 *Turbulence. The legacy of A.N. Kolmogorov.* Cambridge U. Press.

Jiménez, J. 1998 Small scale intermittency in turbulence. *Eur. J. Mech. B/Fluids.* **17,** 405-419.

Jiménez, J. 1999 Intermittency and cascades. *J. Fluid Mech.* in press.

Jiménez, J., Moissy, F., Tabeling, P. and Willaime, H. 1999 Scaling and structure in isotropic turbulence. *Proc. of the I. Newton Inst. Symp. on Intermittency,* June 1999. (C. Vassilicos ed.)

Jiménez, J. and Wray, A.A. 1998 On the characteristics of vortex filaments in isotropic turbulence. *J. Fluid Mech.* **373,** 255-285.

Meneveau, C. & Sreenivasan, K.R. 1991 The multifractal nature of the energy dissipation. *J. Fluid Mech.* **224,** 429-484.

Nelkin, M. 1995 Inertial range scaling of intense events in turbulence. *Phys. Rev. E.* **52,** R4610-4611.

Sreenivasan, K.R. & Dhruva, B. 1998 Self-similarity and coherence in the turbulent cascade. *Prog. Theor. Physics Suppl.* **130,** 103-120.

Van Atta, C.W. & Yeh, T.T. 1975 Evidence for scale similarity of internal intermittency in turbulent flows at large Reynolds numbers. *J. Fluid Mech.* **71,** 417-440.